Long-term post-ovariectomy mouse model recapitulates hypothalamic transcriptomic changes observed during the menopausal transition in women

Authors: Jordana C. B. Bloom[1,2], Encarnacion Torres[2,3]†, Sidney A. Pereira[2,3]†, Liliana Arvizu-Sanchez[2], Audrey N. Fontes[2], Hadine Joffe[3,4], David C. Page[1,5,6], Victor M. Navarro[2,3,7*]

Affiliations:

1. Whitehead Institute for Biomedical Research, Cambridge, MA 02142, USA
2. Division of Endocrinology, Diabetes and Hypertension, Brigham and Women's Hospital, Boston, MA 02115, USA
3. Harvard Medical School, Boston, MA 02115, USA
4. Department of Psychiatry, Beth Israel Deaconess Medical Center, Boston, MA 02115, USA
5. Department of Biology, Massachusetts Institute of Technology, Cambridge, MA 02139, USA
6. Howard Hughes Medical Institute, Cambridge, MA 02142, USA
7. Harvard Graduate Program in Neuroscience, Boston, MA 02115, USA

*Email: vnavarro@bwh.harvard.edu

†These authors contributed equally to this work

Abstract

Menopause significantly impacts women's health, yet hypothalamic changes during this transition remain poorly understood. We analyzed gene expression in human hypothalamic samples across menopausal transition, revealing significant changes in inflammatory pathways, KNDy neuron signaling, and thermoregulatory genes. This analysis also identified novel central markers of menopause, including *AKAP5* and *CDKN1A* (*p21*). To further investigate these changes, we developed a novel mouse model based on long-term (4 months) post-ovariectomy (OVX) that mimics the gonadotropin and temperature fluctuations of menopausal transition. Remarkably, the posterior hypothalamus of 4-month post-OVX mice closely mirrored the transcriptional changes observed in women at the late peri-/early post-menopausal age range (ages 51-55). Both species exhibited increased inflammatory signaling and glial activation, alongside altered KNDy neuron activity. Our findings provide new insights into the central mechanisms of menopausal symptoms and offer a valuable preclinical model for testing interventions.

Introduction

Menopause represents a significant life transition for women, characterized by physiological changes extending beyond reproductive function[1]. Understanding the neurobiological basis of these changes is crucial for advancing women's health and developing targeted interventions for menopausal symptoms[2]. While much attention has been focused on ovarian function, research focused on characterizing the changes that happen at the level of the brain—particularly the hypothalamus—has lagged. The hypothalamus contains neuroendocrine centers that both control and respond to estrogens[3,4], and hypothalamic changes are implicated in disrupted thermoregulation, sleep patterns, and increased mood disorders during menopause[5-12].

Hypothalamic KNDy neurons (expressing kisspeptin, neurokinin B, and dynorphin A) have emerged as central players in vasomotor symptoms (VMS), including hot flashes and night sweats, which are among the most common and disruptive menopausal symptoms[13,14]. The identification of KNDy neurons as VMS triggers has opened new avenues for understanding and treating these symptoms[13,15]. However, our knowledge of broader hypothalamic changes during and after menopause remains incomplete, compounded by limitations in current animal models[16]. By combining human and mouse transcriptomic data, this study enhances our understanding while offering a preclinical platform for developing new approaches to manage menopausal symptoms.

Results

Utilizing publicly available bulk RNA-sequencing data from the Genotype-Tissue Expression (GTEx) project[17], we investigated gene expression changes across the menopausal transition in the human hypothalamus. Female donors with hypothalamic tissue were included in our analyses if they passed GTEx donor eligibility criteria and their sequenced tissue had an RNA integrity number of 6 or greater (Supplementary Table 1). 31 samples from donors including

79 those in the menopausal transition (between the ages of 28 and 65 years old) met our inclusion
80 criteria (Fig. 1a). Surrogate variable analysis (SVA)[18] was performed on the RNA expression
81 matrix prior to gene expression analyses to control for latent, confounding sources of variation in
82 the data, such as postmortem interval, donor cause of death, and hormone therapy status.
83 Additionally, cell type deconvolution of the bulk RNA-sequencing data revealed the presence of
84 previously reported hypothalamic cell types[19] (Supplementary Fig. 1a, Supplementary Table 2)
85 and the presence of all eight major transcription factors (*FEZF1, FOXB1, LHX6, MEIS2, OTP,*
86 *SIM1, SIX3, TBX3*) identified in the human hypothalamus from the HYPOMAP single-nucleus
87 RNA-seq reference atlas[20] (Supplementary Fig. 1b) indicating that there are no major differences
88 in cell type composition between samples in the cohort.

89 Having established that there is comparable cell-type representation across the
90 hypothalamus samples, we next assessed patterns of gene expression changes across the
91 menopausal transition by examining gene expression across age using locally estimated
92 scatterplot smoothing (LOESS). LOESS expression profiles were grouped together based on
93 Euclidean distance hierarchical clustering which revealed distinct patterns across age, including
94 genes with nearly constant (Fig. 1b), decreased (Fig. 1c), and increased (Fig. 1d) expression
95 across age. Of particular interest was the identification of many genes with specific decreases
96 (Fig. 1e) or increases (Fig. 1f) coinciding with expected menopausal transition timing
97 (Supplementary Table 3).

98 Next, we divided the cohort into groups in age bins that correspond to the average age
99 range for each menopausal stage based on large longitudinal studies using the age of final
100 menstrual period as stage-defining factor[21-23] (Fig. 2a). We then performed differential gene
101 expression analyses[24] between groups of donors younger than 45 and those between the ages
102 of 46-50, 51-55, and 56-60. Notably, gene set enrichment analysis (GSEA)[25] revealed the highest
103 and most significant enrichments in inflammatory pathway signaling in the group encompassing
104 donors between the ages of 51-55 (which often includes late peri-menopausal/early post-

105 menopausal individuals) compared to individuals younger than 45 (often pre-menopausal) (Fig.
106 2b and Supplementary Table 4). Furthermore, STRING analysis[26] of TNF-alpha hallmark
107 pathway leading edge genes between the late peri-menopausal/early post-menopausal and pre-
108 menopausal groups highlighted genes previously identified[27,28] to be involved in thermoregulation,
109 including fever responses (Fig. 2c).

110 Given the mounting scientific evidence implicating KNDy neurons in the onset of VMS, we
111 examined the expression of key ligand-receptor systems that constitute the KNDy model, as well
112 as critical regulatory genes, including *TAC1/TACR1* and estrogen receptor α (*ESR1*). We plotted
113 LOESS trajectories of these genes in the human hypothalamus (Fig 2d) to visualize their
114 expression patterns across chronological age. Our analysis revealed that while *KISS1R, TAC3,*
115 *OPRK1*, and *TACR1* did not appear to display major changes with age throughout menopausal
116 transition, they tended to increase after age 50, coinciding with the typical age of menopause.
117 However, *KISS1* and *ESR1* showed a marked increase throughout menopause, as expected due
118 to the decline in circulating estrogen, followed by a decline in expression approximately 10 years
119 after their menopausal peak. The expression of aromatase (*CYP19A1*) showed a progressive
120 increase with age but was unaffected by menopausal transition. Interestingly, the changes in
121 *KISS1* expression were inversely correlated with that of the inhibitory dynorphin (*PDYN*) during
122 this same transition, decreasing during typical menopause years (50-55) and rising shortly after.
123 *TACR3* expression, which is at the center of the mechanistic pathway that triggers VMS, showed
124 a marked increase in the years leading up to menopause, reaching maximum expression at
125 approximately 45 years of age. Thereafter, *TACR3* displayed a constant decrease in expression,
126 reaching minimal levels around 10 years post-menopause (Fig 2d). Additionally, we assessed the
127 expression of *PGR*, *GPER1*, and *ESR2* (Supplementary Fig. 2) based on a recent publication that
128 examined expression of these genes as potential postmortem biomarkers in the hypothalamus[29].

129 We also examined the prostaglandin systems, which are involved in thermoregulation,
130 including fever[27,28]. Prostaglandin synthases 1 and 2 (*PTGS1/2*) increased their hypothalamic

expression with age during post-menopausal years. However, Prostaglandin E receptor 3 (*PTGER3*) increased right after menopause, followed by a sharp decrease around age 60 (Fig 2d). We also observed an increase with age in the expression of translocator protein (*TSPO*), a marker of activated microglia, in late post-menopausal years, as previously reported[30]. Additionally, the pro-inflammatory astrocyte activation markers *GFAP* and *VIM* increase during the years corresponding to the average ages of late peri-/early post-menopause, which aligns with the increase in inflammatory signaling pathways identified in our GSEA (Fig 2b, c).

Based on our identification of thermoregulatory and inflammatory pathway changes during the menopausal transition period, we performed an unbiased approach to identify novel genes of interest. We conducted differential gene expression analysis between age bins corresponding to normal late peri-/early post-menopausal and pre-menopausal periods (Fig. 3a, Supplementary Table 5). We examined expression of the identified significantly differentially expressed genes across the defined age groups (Fig. 3b, Supplementary Table 6) and plotted LOESS trajectories across age for the two identified genes with the most statistically significant adjusted p-values, *AKAP5* and *CDKN1A* (Fig. 2c, d). We used the Allen Brain Cell Atlas Brain Knowledge Platform (https://knowledge.brain-map.org/) to visualize transcript localization in the mouse brain (Supplementary Fig. 3a, b). Additionally, we assessed expression of canonical aging-associated genes[31] across our groups (Supplementary Fig. 4a) and plotted trajectories for genes with previously reported functions in brain aging and cognitive decline[32-36] (Supplementary Fig. 4b, c). Many of the trajectories exhibited notable inflection points during the age range corresponding with late peri-/early post-menopausal years.

To experimentally model the time without estrogen exposure that occurs during reproductive aging, we assessed a series of time points post-OVX in mice (Fig. 4a). Serum luteinizing hormone (LH) concentrations increased progressively compared to the intact model, with levels peaking at 2 months post-OVX before declining at 4 months post-OVX (Fig. 4b). Importantly, this observation mirrors what is observed over the course of reproductive aging in

157 women[21]. To characterize changes in thermoregulation, core temperature was measured across
158 time points in the model with a peak in core temperature observed at 14 days post-OVX (Fig. 4c).
159 The increase in LH and temperature observed at 14 days post-OVX resembles the changes
160 observed in peri- and early menopause in women, while the decline in LH and normalization of
161 core temperature seen at 4 months post-OVX resemble the changes observed in late post-
162 menopausal women.

163 To further characterize this mouse model and determine whether these physiological
164 correlations between the rodent and the human extend to hypothalamic transcriptomic changes,
165 we performed bulk RNA-sequencing of the intact, 14 days (short-term) post-OVX and 4 months
166 (long-term) post-OVX models. We selected two regions of the hypothalamus to sequence based
167 on the localization of neurons controlling temperature regulation (preoptic area, POA) and the
168 localization of neurons controlling the metabolic and reproductive centers (posterior
169 hypothalamus, PH). Cell type deconvolution analyses of the bulk RNA-sequencing data revealed
170 the presence of previously reported hypothalamic cell types[19] across all samples just as in the
171 human dataset (Supplementary Fig. 5).

172 Global gene set enrichment analysis revealed the greatest enrichment in inflammatory
173 pathways similar to what we identified in the human hypothalamus (Fig. 4d, Supplementary Table
174 7). STRING analysis[26] of TNF-alpha hallmark pathway leading edge genes in the POA also
175 identified genes related to thermoregulation (Supplemental Fig. 6). We then conducted
176 differential gene expression[24] analyses between intact, short-term and long-term post-OVX
177 models in both the PH and POA. Volcano plots highlight significantly differentially expressed
178 genes between labeled conditions and regions (Fig. 4e-h, Supplemental Fig. 7a and b,
179 Supplementary Table 8), with heatmaps showing how the identified genes are expressed across
180 conditions in the PH (Fig. 4i) and POA (Fig. 4j) (Supplementary Table 9). Among the differentially
181 expressed genes, *Gm28040*, which shares overlapping CDS with *Kiss1*, shows the largest
182 expression change, which was increased at 14 days and 4 month OVX in the PH and decreased

183 in both groups in the POA, resembling the known regulation of *Kiss1* in both hypothalamic areas[37].
184 This suggests that in the mouse, *Gm28040* encodes a kisspeptin isoform (Fig 4 e-h,
185 Supplementary Table 8).

186 Next, we examined the expression of previously identified marker genes for reproduction,
187 thermoregulation, and inflammation (particularly related to astrocyte and microglia activity) in both
188 the PH (Supplemental Fig. 8a) and the POA (Supplemental Fig. 8b), as we performed previously
189 in human transcriptomic samples (Fig 2). While none of the genes reached statistical significance
190 after adjusting for multiple hypothesis testing, the expression of inflammation and astrocytic
191 markers from gonad intact to 4 months post-OVX showed similar increasing trends to that
192 observed in the human hypothalamus across menopausal transition, with notable increases in
193 *Vim*, *Iba1*, and *Tspo* in the PH, and in the prostaglandin pathway (*Ptgs2*) in the POA. The KNDy
194 genes, involved in reproductive and thermoregulatory (VMS) control, are highly regulated by sex
195 steroids[38], and thus they showed the expected increase in expression in the PH (where the
196 arcuate nucleus is located) in proportion to time after OVX.

197 A substantial proportion of expressed genes are shared between the human and mouse
198 hypothalamus (~77%; Supplementary Fig. 9). Comparison of the GSEA results between the
199 human GTEx dataset and OVX mouse model revealed statistically significant pathway enrichment
200 correlations between the two datasets (Fig. 5a), further supporting the suitability of this mouse
201 model to study hypothalamic changes during the menopausal transition. We also compared
202 GSEA results between our OVX mouse model and a published single-cell RNA-seq dataset of
203 the aging female mouse hypothalamus[19] to assess whether the mouse models capture similar
204 hypothalamic gene expression changes. Of the 26 Hallmark pathways significantly impacted in
205 the human dataset (Fig. 2b, Supplementary Table 4) only eight were similarly altered in the aged
206 mouse hypothalamus[19], compared with 14 in the OVX model. Notably, the aged mouse study[19]
207 did not report any changes in the estrogen response or TNFα signaling pathways, which are
208 consistently affected in both the human dataset and the OVX mouse model and highly relevant

209 to the menopausal transition[39]. At the cell-type level, the observed pathway changes in
210 macrophages and microglia from the aged mouse hypothalamus dataset exhibited the greatest
211 similarity to those changes observed in the human and OVX mouse model (Supplementary Table
212 10). Despite this partial overlap between mouse models, the two only share a single significantly
213 differentially expressed gene in common (*Thsd4)*, suggesting that they capture largely distinct
214 hypothalamic transcriptional programs.

215 To determine whether the cross-species similarities extend beyond pathway-level
216 analyses to individual genes, we selected *TACR3*, which has a documented role in the onset and
217 severity of VMS[40] and performed co-expression analyses to identify genes whose expression
218 positively correlates with *TACR3* (in human) or *Tacr3* (in the OVX mouse model). These
219 correlations revealed statistically significant overlap in the positively regulated genes with *TACR3*
220 in the two species (Fig. 5b, Supplementary Table 11). We then hypothesized that if the short and
221 long term OVX mouse model is a suitable model to study hypothalamic transcriptomic changes
222 throughout menopause, the differentially expressed genes identified in the human samples should
223 show similar trends in our mouse model and vice versa. We depicted gene expression across the
224 groups as heatmaps, which show differentially expressed genes from the human dataset across
225 mouse conditions (Fig. 5c, d) and mouse PH and POA datasets across human age groups (Fig.
226 5e, f). Remarkably, two-thirds of the differentially expressed genes identified in the human
227 between 51-55 years showed a clear increase at 4 months post-OVX, while the remaining one-
228 third were captured at 14 days post-OVX in both PH and POA. The opposite analysis revealed a
229 majority of the genes that presented the highest changes at 4 months post-OVX were upregulated
230 in the 51-55 year old age group, usually corresponding to individuals in the late peri-/early post-
231 menopausal stage.

232 In sum, these findings indicate that the short-term and long-term post-OVX mouse models
233 described can be used as an experimental system to model hypothalamic changes in menopausal
234 women with a high degree of fidelity. Furthermore, our data reveal that while LH changes occur

235 relatively fast after OVX, the majority of hypothalamic transcriptomic changes that correlate with
236 perimenopause are not evident until 4 months post OVX (Figs 4, 5a). These data also reveal that
237 the mouse PH resembles the whole human hypothalamus better than the mouse POA.

238 Further characterization of this mouse model was carried out at the protein level. To this
239 end, we continued our focus on the hypothalamic NKB/NK3R system. Unlike *Tac2* expression,
240 which increases with time after OVX (Supplemental Fig. 8), the expression of NKB decreased
241 after OVX (Supplemental Fig. 10). This effect is expected for highly released neuropeptides,
242 suggesting that this ligand is actively being released rather than stored. To assess the activity of
243 the arcuate nucleus (site of KNDy neurons) after OVX, we stained for the early activation marker
244 cFos. This assay revealed that cFos expression in the arcuate nucleus is significantly lower at 4
245 months compared to 14 days post-OVX, and this was correlated with an increase in inflammation,
246 as shown by Gfap staining, which correlates with the findings observed in human and mouse
247 transcriptomes. Nonetheless, these data could not answer whether the decrease in activity was
248 also at the level of the KNDy neuron or due to changes in other cells of the arcuate. Thus, we
249 quantified the changes in cFos within NKB neurons, which revealed a 50% decrease in NKB
250 neuron activation.

251

252 **Discussion**

253 Our study utilizes transcriptomics from human hypothalamic samples across adult ages
254 to identify specific gene expression trends associated with aging and the menopausal transition
255 in women. Overall, our findings offer new genome-wide insights into the complex molecular
256 landscape of the aging hypothalamus and its response to declining ovarian function.

257 A key finding from our analysis is the increased inflammatory signaling in the
258 hypothalamus during the age range usually corresponding to individuals in late peri-/early post-
259 menopause, consistent with the concept of "inflammaging" that develops with advanced age and
260 contributes to various age-related pathologies[41]. Gene set enrichment analysis revealed

261 significant upregulation of inflammatory pathways, particularly TNF-alpha signaling via NF-κB,
262 during this transition period (Fig. 2b). Our STRING analysis of differentially expressed genes
263 highlighted several that are involved in thermoregulation and fever responses (Fig. 2c), providing
264 a potential mechanistic link between hypothalamic inflammation and vasomotor symptoms
265 commonly experienced during menopause. This neuroinflammatory signature was further
266 evidenced by increased expression of astrocyte activation markers *GFAP* and VIM during normal
267 early post-menopause years, as well as the microglial marker *TSPO* in late post-menopausal
268 years (Fig. 2d). Additionally, we observed age-associated increases in prostaglandin synthesis
269 enzymes *PTGS1/2*, which may contribute to neuroinflammation and altered pain sensitivity in
270 older women. Importantly, our mouse ovariectomy model recapitulated these inflammatory
271 changes, with gene set enrichment analysis showing significant enrichment of inflammatory
272 pathways at 4 months post-OVX (Fig. 4d), closely matching our findings in the late peri-/early
273 post-menopausal women. These hypothalamic inflammatory and glial changes may have
274 functional consequences extending beyond the central nervous system. Activated astrocytes and
275 microglia in thermoregulatory and metabolic hypothalamic nuclei can modulate local neuronal
276 excitability through altered neurotransmitter reuptake, gap junction coupling or cytokine release
277 [42]. The prostaglandin pathway changes we observed (*PTGS1/2, PTGER3*) directly link to
278 autonomic output controlling cutaneous vasodilation, which is the effector mechanism of VMS
279 [43,44]. Furthermore, hypothalamic inflammation can influence systemic metabolic regulation
280 through altered brown adipose tissue thermogenesis and energy expenditure, potentially
281 contributing to the weight gain and metabolic dysregulation commonly observed during the
282 menopausal transition [44,45]. The upregulation of NF-κB-mediated inflammatory signaling in the
283 hypothalamus may also propagate to peripheral tissues through neuroendocrine and autonomic
284 pathways, contributing to the systemic low-grade inflammation ("inflammaging") associated with
285 increased cardiometabolic risk in postmenopausal women [46]. While our study identifies these

286 pathways as correlatively altered, future mechanistic studies using the OVX model that we
287 describe could directly test these hypothesized central-peripheral links.

288 We also assessed the changes in the expression of genes involved in reproductive
289 function and thermoregulation across the menopausal transition. As expected, *KISS1* expression
290 increased markedly during menopause[47,48], likely due to loss of estrogen negative feedback,
291 followed by a decline approximately 10 years post-menopause (Fig. 2d). This late-life reduction
292 in kisspeptin signaling may contribute to the eventual decline in gonadotropin levels seen years
293 after menopause onset[49,50]. Intriguingly, *TACR3* expression, which GWAS studies have
294 associated with the severity of VMS[40], showed a distinct pattern, increasing in the years leading
295 up to menopause, peaking around age 45, and then progressively declining (Fig. 2d). Given the
296 proposed role of neurokinin B signaling in triggering vasomotor symptoms[15,51], this expression
297 pattern aligns well with the typical time course of hot flashes, which often begin in perimenopause
298 and resolve within 5-10 years [52]. Thus, our data offer novel insights into the mechanisms that
299 could mediate the decrease in LH levels and termination of hot flashes years after menopause,
300 likely mediated by the significant drop in hypothalamic *KISS1* and *TACR3* expression.

301 Unbiased differential expression analysis identified two genes, *AKAP5* and *CDKN1A*, as
302 particularly notable markers of the menopausal transition (Fig. 3a-d). *AKAP5* (A-kinase anchoring
303 protein 5) encodes a scaffolding protein involved in synaptic plasticity[53-56] and showed decreased
304 expression in late peri-/early post-menopause ages. *CDKN1A*, encoding the cell cycle regulator
305 p21,[57] was upregulated in late peri-/early post-menopause ages. Interestingly, p21 has been
306 implicated in promoting senescence-associated secretory phenotype (SASP)[57-60], in which
307 senescent cells increase the secretion of inflammatory factors, thus potentially contributing to the
308 inflammatory phenotype we observed. The identification of *CDKN1A* (p21) upregulation in the 51-
309 55 age range suggests that cellular senescence may contribute to hypothalamic aging. Whether
310 this effect is mediated by p21 action at the glial level to promote senescence remains to be
311 investigated.

312 To determine whether these human transcriptomic changes could be modeled
313 experimentally, we developed a mouse ovariectomy (OVX) model with both short-term (14 day)
314 and long-term (4 month) timepoints. Remarkably, we found that the 4-month post-OVX timepoint
315 recapitulated many key features of the human menopausal transition. LH levels showed an initial
316 increase followed by decline (Fig. 4b), mirroring the menopausal transition[21] in humans. Core
317 body temperature was elevated at 14 days post-OVX but normalized by 4 months (Fig. 4c),
318 paralleling the typical time course of vasomotor symptoms[52]. Transcriptomic analysis of the
319 mouse PH and POA revealed striking similarities to the human dataset. Gene set enrichment
320 analysis showed significant enrichment of inflammatory pathways at 4 months post-OVX (Fig.
321 4d), closely matching our findings in women undergoing the menopausal transition. Importantly,
322 cross-species comparison demonstrated significant correlation between the transcriptomic
323 changes in our human and mouse datasets (Fig. 5a). Nearly two-thirds of genes differentially
324 expressed in women at age ranges between normal late peri-/early post-menopause and pre-
325 menopause showed concordant changes at 4 months post-OVX in mice, particularly at the level
326 of the PH. This high degree of conservation suggests that our long term OVX model effectively
327 captures key molecular features of the human menopausal transition.

328 To further validate our model, we examined protein changes in neurokinin B (NKB)
329 expression and neuronal activation. Immunofluorescence staining revealed decreased NKB
330 levels in the arcuate nucleus at both 14 days and 4 months post-OVX (Supplemental Fig. 10a-
331 c,j). This contrasts with the increased *Tac2* mRNA expression we observed and suggests
332 enhanced NKB release and depletion of peptide stores. Importantly, we found reduced c-Fos
333 expression in NKB neurons at 4 months post-OVX (Supplemental Fig. 10m,n), indicating
334 decreased neuronal activity. This aligns with the declining *TACR3* expression seen in
335 postmenopausal women and may reflect adaptive changes to prolonged estrogen deficiency.

336 Of note, while multiple rodent models exist to study menopausal biology, we selected long-
337 term OVX for this study because it provides precise control over the timing of estrogen withdrawal,

338 enabling direct alignment of endocrine, thermoregulatory, and transcriptomic changes with human
339 age-associated windows. The VCD (4-vinylcyclohexene diepoxide) model offers an alternative
340 approach that more closely mimics gradual follicular depletion characteristic of spontaneous
341 menopause. However, VCD induces variable timing of ovarian failure (typically 15-160 days
342 depending on dose and strain)[61], residual ovarian interstitial tissue can produce androgens for
343 months[61-63] and repeated dosing and potential off-target effects add variables that are absent in
344 OVX[64,65]. Our OVX model, while representing abrupt surgical menopause, provides a robust and
345 widely validated framework for studying chronic hypoestrogenism and serves as a complementary
346 approach to gradual-depletion models. This model also provides a platform for future studies
347 examining whether estrogen replacement reverses specific transcriptomic changes associated
348 with menopausal-like transitions in the mouse that could be translated into humans.

349 In conclusion, this study serves as a valuable resource for future investigations into
350 hypothalamic aging and the menopausal transition. We demonstrate that our OVX mice model
351 can provide a physiologically relevant platform for experimental manipulations to determine the
352 functional significance of specific molecular changes observed in the human samples. Together,
353 these insights and tools pave the way for a deeper understanding of menopause and the
354 development of interventions that could significantly improve women's health during this life stage.
355 Nonetheless, several limitations should be considered when interpreting our findings. First, both
356 human and mouse analyses relied on bulk RNA-sequencing, which captures population-averaged
357 gene expression but cannot resolve cell-type-specific transcriptomic changes. While we
358 employed marker-based deconvolution approaches using the Hajdarovic et al. single-cell
359 reference dataset [66], these methods provide estimates rather than direct measurements of cellular
360 composition changes. In this context, the recent publication of comprehensive human
361 hypothalamic single-cell atlases [67,68] provides an important resource for future studies aimed at
362 characterizing cell-type-specific responses to menopause. Second, protein-level validation in our
363 study focused on NKB, c-Fos, and GFAP immunostaining in the mouse model. While

364 transcriptomic changes provide insight into cellular responses, post-transcriptional regulation may
365 result in discordance between mRNA and protein levels, particularly for secreted neuropeptides
366 where release dynamics affect detectable protein stores, as observed for NKB. Third, the human
367 GTEx dataset presents inherent confounders including variation in postmortem interval, unknown
368 hormone therapy history, and heterogeneous causes of death. We addressed latent sources of
369 variation computationally using Surrogate Variable Analysis (SVA), but cannot fully account for
370 unmeasured biological and technical variables.
371
372 **Materials and Methods**
373 **Mouse studies**
374 *Study approval and animals*
375 The animal studies were approved by the Brigham and Women's Hospital Institutional
376 Animal Care and Use Committee (IACUC) in the Center for Comparative Medicine. Adult wild-
377 type (WT) C57/BL6 female mice were group housed under constant conditions of temperature
378 (22–24°C) and light (12:12-hour light:dark cycle), fed with standard mouse chow and ad libitum
379 access to tap water.
380
381 *Experimental design*
382 To investigate the effects of sex steroids withdrawal on LH levels, core temperature (Tc),
383 and hypothalamic transcriptome profile, intact WT female mice were bilaterally ovariectomized
384 (OVX) to generate mouse models that would resemble pre-menopause, menopause transition
385 and early post-menopause in women. Blood LH levels and Tc were measured at baseline, when
386 females were still intact, at 7-, 14- and 21-days post OVX and at 1-, 2- and 4-months post OVX.
387 Additional females were euthanized before OVX in diestrus (pre-menopause group), after 14 days
388 of OVX (menopause transition group) or after 4 months of OVX (early post-menopause group)

389 and their posterior (PH) and preoptic area (POA) of the hypothalamus were collected for
390 transcriptome profile analysis by bulk RNA-seq.
391
392 *Ovariectomy (OVX)*
393 Adult (3-4 months-old) female mice were bilaterally OVX under isoflurane anesthesia.
394 Mice were treated with Buprenex SR (0.1 mg/kg, SC) and meloxicam (5 mg/kg, SC) on the day
395 of surgery. Mice were allowed to recover for at least 1 week before the start of experiments.
396
397 *Whole blood samples and LH ELISA*
398 For LH measurements, a 4µl blood sample was collected with a pipette. Whole blood was
399 immediately diluted in 116µl of 0.05% PBST [phosphate buffer saline (Boston Bio Products,
400 catalog #BM220) containing Tween-20 (Sigma, catalog #P2287)], vortexed, and frozen on dry ice.
401 Samples were stored at 80˚C until analyzed using an in-house sandwich enzyme-linked
402 immunosorbent assay as previously described Kreisman, et al. [69].
403
404 *Core temperature (Tc)*
405 For Tc measurements, intact female mice were implanted (intraperitoneally) with an IPTT-
406 300 temperature transponder (BioMedic Data Systems, Inc.). Tc from the transponder were
407 collected with a DAS-8007 Reader and DASHost 8000 software (BioMedic Data Systems, Inc.).
408
409 *Immunohistochemistry*
410 Animals were anesthetized with a ketamine/xylazine/saline cocktail and transcardially
411 perfused with saline (0.9% NaCl) followed by 4% paraformaldehyde (PFA) diluted in phosphate
412 buffer (PB) (Boston BioProducts, Inc). Brains were removed, stored in 4% PFA overnight and then
413 transferred into sucrose solution (30% sucrose in 0.1 M PB, Thermo Fisher Scientific) at 4˚C. After
414 sucrose infiltration, the tissue was frozen in Tissue-Tek® O.C.T. Compound (Sakura® Finetek-

415 4583) and cut on a freezing stage microtome (Microm HM 450, Thermo Fisher Scientific) into 30
416 µm coronal sections. Free-floating sections were washed in tris buffered saline (TBS, Boston
417 BioProducts, Inc) and blocked for 1 hour at room temperature in incubation solution [TBS +
418 0.3%Triton™ X-100 (Millipore Sigma) + 2% normal goat serum (NGS)]. Sections were
419 subsequently incubated for 48 hours at 4˚C with primary antibodies: rabbit-anti neurokinin B
420 (1:1000, Novus Biologicals, catalog #NB300-201), guinea pig anti-cFos (1:1000, Synaptic
421 System, catalog #226308) and mouse anti-GFAP (1:300, Cell Signaling, catalog #3670) diluted
422 in incubation solution. Next, sections were incubated for 1 hour at room temperature with
423 secondary antibodies: anti-rabbit Alexa Fluor 594 (1:500, Thermo Fisher Scientific, catalog
424 #A11012), anti-guinea pig Alexa Fluor 488 (1:500, Jackson ImmunoResearch, catalog
425 #706545148) and anti-mouse donkey Alexa 594 (1:500, Invitrogen, catalog #A32744). Sections
426 were mounted onto Super-frost plus glass slides (Fisher Laboratories), air dried and cover slipped
427 with Vectashield mounting medium with DAPI (Vector laboratories).
428
429 *Microscopy and image analysis*
430 The images were captured by using a fluorescent microscope (Leica DM 2500) in JPG
431 format and processed using the open-source software ImageJ, Fiji (National Institutes of Health,
432 Bethesda, Maryland). For image quantification, representative images of the areas of interest (i.e.,
433 ARC) were delimited using as reference the mouse section from Allen Brain Atlas [70]. Both sides
434 of bilateral ARC were counted on a similar number of sections and animal, and replicate values
435 were averaged.
436
437 *RNA extraction, library preparation, and sequencing*
438 Mouse posterior hypothalamus and preoptic area regions were dissected and flash frozen
439 prior to extracting RNA using a Zymo Quick RNA microprep kit according to the manufacturer's
440 instructions. RNA concentration was measured using a Qubit 4.0 fluorometer and the Quibit RNA

441 HS Assay Kit (ThermoFisher). All samples had RNA integrity numbers (RIN) greater than 7 as
442 measured on a Bioanalyzer 2100 instrument (Aligent). RNA sequencing libraries were prepared
443 using the KAPA mRNA HyperPrep–Stranded Kit (Roche) and sequenced on a NovaSeq SP
444 (Illumina) with 50bp paired-end reads.
445
446 *RNA-seq data processing and analysis*
447 We performed all analyses using mouse genome build mm39. To pseudoalign reads to
448 the transcriptome annotation and estimate expression levels of each transcript, we used kallisto[71]
449 in the tximport package[72] (v1.24.0). We imported the resulting count data (abundance.h5 file) into
450 R for analysis in DESeq2[24] (v1.36.0). To adjust for unknown, unmodeled or latent sources of
451 noise in the data we performed surrogate variable analysis (SVA) using the smartSVA package[18]
452 (v0.1.3) and used SV1 as a covariate in the differential gene expression analysis. Both
453 pseudoalignment and DESeq2 were performed on the entire transcriptome annotation, but, in
454 some cases, we restricted our downstream analysis to protein-coding genes, as annotated in
455 GENCODE version M30[73]. For gene set enrichment analysis (GSEA), we performed analyses
456 on pre-ranked ordered gene lists using the fgsea package[25] (v1.22.0).
457
458 *Prediction of protein interactions*
459 The first 30 leading edge genes from the comparison of the POA between female gonadal
460 intact vs. 4-month post-OVX mice were selected as the target gene list for TNF-α signaling
461 through NF-κB. The gene list was imported into STRING[74] for network reconstruction,
462 visualization and enrichment analysis [74]. Medium confidence, as the minimum required interaction
463 scored, was selected (0.400). Enrichment biological processed defined by gene ontology (GO)
464 were assessed. Of the top 10 variables identified by the GO terms, highlighted genes related to
465 thermoregulation and inflammation response to menopause transition are shown.

466

467 **Human studies**

468 *Human hypothalamus inclusion criteria*

469 Bulk RNA-sequencing read count data from human hypothalamus tissue was obtained
470 from publicly available Genotype-Tissue Expression (GTEx) Project[17] data. We included donor
471 tissue as part of our dataset if a sample met the following criteria: 1) donor eligibility criteria
472 (INCEXC) == TRUE, 2) tissue RNA quality score (RIN) >= 6, 3) donors were female (SEX == 2).

473

474 *Sex and Gender Reporting*

475 All human hypothalamic samples from the GTEx database were from donors recorded as
476 female (biological sex). This study specifically focuses on women's health, examining
477 transcriptomic changes across the female reproductive lifespan from premenopausal through
478 postmenopausal years. Sex was determined by GTEx based on donor records. We use the term
479 "women" throughout to reflect the clinical population most directly affected by natural menopause,
480 while acknowledging that individuals of diverse gender identities with intact ovarian function may
481 also experience menopausal transition.

482

483 *Human data analysis*

484 After the sub-setting the GTEx RNA expression file for our samples of interest, we adjusted
485 for unknown, latent sources of noise in the data using SVA with the smartSVA package[18] (v0.1.3).
486 Differential expression analyses across age bins were performed using DESeq2[24] (v1.36.0) and
487 GSEA was performed on pre-ranked ordered gene lists using the fgsea package[25] (v1.22.0).
488 Gene expression trajectories across age (and parallel analyses across OVX conditions in mouse)
489 were performed on protein-coding genes using locally estimated scatterplot smoothing (LOESS)
490 similarly to Piehl et al. 2022[75]. Gene level output from LOESS across age was subjected to
491 expression trajectory correlation analysis. Genes were ranked based on their correlation with the

492 *TACR3/Tacr3* expression pattern. STRING interaction analyses were performed as described
493 above. Given the unavailability of hormone measurements in GTEx, we used chronological age
494 bins as proxies for reproductive stage, informed by epidemiological data from the Study of
495 Women's Health Across the Nation (SWAN) where median age at final menstrual period is 51-52
496 years[76]. Samples were grouped into five age ranges: <45 years (corresponding to typical
497 premenopausal years), 46-50 years (early perimenopausal age range), 51-55 years (late peri-
498 /early postmenopausal age range), 56-60 years (postmenopausal years), and 61-65 years (late
499 postmenopausal years). We acknowledge that individual variation in menopausal timing means
500 our age-based classification of human samples represents chronological age bins that correspond
501 to typical pre-, peri-, and postmenopausal years in population studies, but we cannot definitively
502 assign clinical menopausal staging or vasomotor symptom status to individual donors. The GTEx
503 consortium did not collect serum samples, precluding direct hormone measurements or
504 application of recently developed gene-based menopausal biomarkers.
505
506 *Cell type decomposition analysis*
507 We performed cell type decomposition analyses to estimate the cell type composition of
508 our bulk RNA-seq datasets from human and mouse using the BisqueRNA package[77] (v1.0.5).
509 Table S2 lists the marker genes used to annotation cell types[19].
510
511 *Quantification and statistical analyses*
512 Various statistical tests were used to calculate p values as indicated in the methods
513 section, figure legends, or text, where appropriate. All statistics were calculated using R software,
514 version 4.2.1 unless stated otherwise. Differential gene expression was performed using DESeq2
515 with Benjamini-Hochberg false discovery rate (FDR) correction; genes with adjusted p-values <
516 0.05 were considered significant. Prior to DE analysis, we performed Surrogate Variable Analysis
517 (SVA) using the smartSVA package to adjust for unknown latent sources of variation in both

human and mouse datasets. Gene set enrichment analysis (GSEA) was performed using the fgsea package on pre-ranked gene lists, with FDR-corrected normalized enrichment scores (NES) reported. LOESS trajectory analysis was adapted from Piehl et al. 2022 to visualize continuous expression patterns across age; genes with similar trajectories were identified by hierarchical clustering using Euclidean distance. Statistical comparisons of physiological measurements (LH, core temperature) and immunofluorescence quantification used one-way ANOVA with Tukey's post-hoc test or Mann-Whitney U test as appropriate. $P < 0.05$ or $FDR < 0.05$ was considered statistically significant.

Funding

This work has been supported by the National Institutes of Health (NIH) grant HD090151, DK133760, HD099084 and NIH Research Grant U54 AG062322 (ROSA Center) funded by The National Institute on Aging (NIA) and Office of Research on Women's Health (ORWH) to (ETJ, SAP, LAS, ANF, VMN), The Brit Jepson d'Arbeloff Center on Women's Health (JCBB, DCP)

Author contributions

Conceptualization: JCBB, ETJ, SAP, VMN

Methodology: JCBB, ETJ, SAP, LAS, ANF

Investigation: JCBB, ETJ, SAP

Visualization: JCBB, ETJ, SAP

Supervision: DCP, VMN

Writing—original draft: JCBB, VMN

Writing—review & editing: JCBB, ETJ, SAP, HJ, DCP, VMN

Competing interests Authors declare that they have no competing interests.

Data and materials availability:

- Raw RNA-seq data from mouse posterior hypothalamus and preoptic area regions have been deposited to dbGAP and are publicly available as of the date of publication.
- This paper analyzes existing, publicly available GTEx consortium data available on the GTEx Portal (https://www.gtexportal.org/home/).
- Original code to perform analyses has been deposited at Github and is publicly available as of the date of publication.
- Any additional information required to reanalyze the data reported in this study is available from the lead contact upon request.

References

1 Davis, S. R. *et al.* Menopause. *Nature Reviews Disease Primers* **1**, 15004 (2015). https://doi.org/10.1038/nrdp.2015.4

2 Brinton, R. D., Yao, J., Yin, F., Mack, W. J. & Cadenas, E. Perimenopause as a neurological transition state. *Nature reviews. Endocrinology* **11**, 393-405 (2015). https://doi.org/10.1038/nrendo.2015.82

3 Rance, N. E. & Uswandi, S. V. Gonadotropin-releasing hormone gene expression is increased in the medial basal hypothalamus of postmenopausal women. *J Clin Endocrinol Metab* **81**, 3540-3546 (1996). https://doi.org/10.1210/jcem.81.10.8855798

4 Herbison, A. E. in *Physiology of Reproduction* (ed J. Neil and E. Knobil) 1415–1482 (Academic Press, 2006).

5 Ameratunga, D., Goldin, J. & Hickey, M. Sleep disturbance in menopause. *Intern Med J* **42**, 742-747 (2012). https://doi.org/10.1111/j.1445-5994.2012.02723.x

6 Augoulea, A. *et al.* Psychosomatic and vasomotor symptom changes during transition to menopause. *Prz Menopauzalny* **18**, 110-115 (2019). https://doi.org/10.5114/pm.2019.86835

7 Coborn, J. *et al.* Disruption of Sleep Continuity During the Perimenopause: Associations with Female Reproductive Hormone Profiles. *J Clin Endocrinol Metab* **107**, e4144-e4153 (2022). https://doi.org/10.1210/clinem/dgac447

8 Cohn, A. Y. *et al.* Effects of Sleep Fragmentation and Estradiol Decline on Cortisol in a Human Experimental Model of Menopause. *J Clin Endocrinol Metab* **108**, e1347-e1357 (2023). https://doi.org/10.1210/clinem/dgad285

9 Greendale, G. A., Karlamangla, A. S. & Maki, P. M. The Menopause Transition and Cognition. *JAMA* **323**, 1495-1496 (2020). https://doi.org/10.1001/jama.2020.1757

10 Kravitz, H. M. J., H. . Sleep during the perimenopause: a SWAN story. *Obstet Gynecol Clin North Am* **38**, 567-586 (2011).

11 Landis, C. A. & Moe, K. E. Sleep and menopause. *Nurs Clin North Am* **39**, 97-115 (2004). https://doi.org/10.1016/j.cnur.2003.11.006

12 Reed, S. D., Newton, K. M., LaCroix, A. Z., Grothaus, L. C. & Ehrlich, K. Night sweats, sleep disturbance, and depression associated with diminished libido in late menopausal transition and early postmenopause: baseline data from the Herbal Alternatives for Menopause Trial (HALT). *Am J Obstet Gynecol* **196**, 591-597 (2007).

13 Koysombat, K., McGown, P., Nyunt, S., Abbara, A. & Dhillo, W. S. New advances in menopause symptom management. *Best Pract Res Clin Endocrinol Metab* **38**, 101774 (2024). https://doi.org/10.1016/j.beem.2023.101774

14 Freeman, E. W., Sammel, M. D., Lin, H., Liu, Z. & Gracia, C. R. Duration of menopausal hot flushes and associated risk factors. *Obstet Gynecol* **117**, 1095-1104 (2011). https://doi.org/10.1097/AOG.0b013e318214f0de

15 Prague, J. K. *et al.* Neurokinin 3 receptor antagonism as a novel treatment for menopausal hot flushes: a phase 2, randomised, double-blind, placebo-controlled trial. *Lancet* **389**, 1809-1820 (2017). https://doi.org/10.1016/S0140-6736(17)30823-1

16 Koebele, S. V. & Bimonte-Nelson, H. A. Modeling menopause: The utility of rodents in translational behavioral endocrinology research. *Maturitas* **87**, 5-17 (2016). https://doi.org/10.1016/j.maturitas.2016.01.015

17 Lonsdale, J. *et al.* The Genotype-Tissue Expression (GTEx) project. *Nature Genetics 2013 45:6* **45** (2013-05-29). https://doi.org/10.1038/ng.2653

18 Chen, J. *et al.* Fast and robust adjustment of cell mixtures in epigenome-wide association studies with SmartSVA - PubMed. *BMC genomics* **18** (05/26/2017). https://doi.org/10.1186/s12864-017-3808-1

19 Hajdarovic, K. H. *et al.* Single-cell analysis of the aging female mouse hypothalamus. *Nature Aging 2022 2:7* **2** (2022-07-04). https://doi.org/10.1038/s43587-022-00246-4

20 Tadross, J. A. *et al.* A comprehensive spatio-cellular map of the human hypothalamus. *Nature* **639** (2025 Feb 5). https://doi.org/10.1038/s41586-024-08504-8

21 Soares, A. G. *et al.* Longitudinal changes in reproductive hormones through the menopause transition in the Avon Longitudinal Study of Parents and Children (ALSPAC). *Scientific Reports 2020 10:1* **10** (2020-12-04). https://doi.org/10.1038/s41598-020-77871-9

22 Khoudary, S. R. E. *et al.* The menopause transition and women's health at midlife: a progress report from the Study of Women's Health Across the Nation (SWAN). *Menopause (New York, N.y.)* **26** (2019/10). https://doi.org/10.1097/GME.0000000000001424

23 Gold, E. B. *et al.* Factors related to age at natural menopause: longitudinal analyses from SWAN. *Am J Epidemiol* **178**, 70-83 (2013). https://doi.org/10.1093/aje/kws421

24 Love, M. I. *et al.* Moderated estimation of fold change and dispersion for RNA-seq data with DESeq2. *Genome Biology 2014 15:12* **15** (2014-12-05). https://doi.org/10.1186/s13059-014-0550-8

25 Korotkevich, G. *et al.* Fast gene set enrichment analysis. *BioRxiv* (2021-02-01). https://doi.org/10.1101/060012

26 The STRING database in 2021: customizable protein-protein networks, and functional characterization of user-uploaded gene/measurement sets - PubMed. *Nucleic Acids Res* **49** (01/08/2021). https://doi.org/10.1093/nar/gkaa1074

27 Blomqvist, A. & Engblom, D. Neural Mechanisms of Inflammation-Induced Fever. *The Neuroscientist* **24** (2018/08). https://doi.org/10.1177/1073858418760481

28 Prostaglandin production selectively in brain endothelial cells is both necessary and sufficient for eliciting fever - PubMed. *Proc Natl Acad Sci USA* **119** (10/25/2022). https://doi.org/10.1073/pnas.2122562119

29 Tickerhoof, M. *et al.* Postmortem tissue biomarkers of menopausal transition. *Molecular psychiatry* (2025 Aug 27). https://doi.org/10.1038/s41380-025-03177-9

30 Butler, T. *et al.* Positron Emission Tomography reveals age-associated hypothalamic microglial activation in women. *Sci Rep* **12**, 13351 (2022). https://doi.org/10.1038/s41598-022-17315-8

31 Tacutu, R. *et al.* Human Ageing Genomic Resources: new and updated databases. *Nucleic Acids Res* **46** (2018/01/01). https://doi.org/10.1093/nar/gkx1042

32 O'Day, D. H. Calmodulin Binding Proteins and Alzheimer's Disease: Biomarkers, Regulatory Enzymes and Receptors That Are Regulated by Calmodulin. *Int J Mol Sci* **21** (2020/10). https://doi.org/10.3390/ijms21197344

33 Kim, J., Basak, J. M. & Holtzman, D. M. The Role of Apolipoprotein E in Alzheimer's Disease. *Neuron* **63** (2009/08/13). https://doi.org/10.1016/j.neuron.2009.06.026

34 Bateman, R. J. *et al.* Clinical and Biomarker Changes in Dominantly Inherited Alzheimer's Disease. *New England Journal of Medicine* **367** (2012-08-30). https://doi.org/10.1056/NEJMoa1202753

35 SIRT1 in Neurodevelopment and Brain Senescence. *Neuron* **81** (2014/02/05). https://doi.org/10.1016/j.neuron.2014.01.028

36 Catechol-O-methyltransferase polymorphisms and some implications for cognitive therapeutics - PubMed. *NeuroRx : the journal of the American Society for Experimental NeuroTherapeutics* **3** (2006 Jan). https://doi.org/10.1016/j.nurx.2005.12.010

37 Smith, J. T., Cunningham, M. J., Rissman, E. F., Clifton, D. K. & Steiner, R. A. Regulation of Kiss1 gene expression in the brain of the female mouse. *Endocrinology* **146**, 3686-3692 (2005). https://doi.org/10.1210/en.2005-0488

38 Goodman, R. L., Herbison, A. E., Lehman, M. N. & Navarro, V. M. Neuroendocrine control of gonadotropin-releasing hormone: Pulsatile and surge modes of secretion. *J Neuroendocrinol* **34**, e13094 (2022). https://doi.org/10.1111/jne.13094

39 J, P., R, K., M, P. & H, S. Changes in proinflammatory cytokine activity after menopause - PubMed. *Endocr Rev* **23** (2002 Feb). https://doi.org/10.1210/edrv.23.1.0456

40 Crandall, C. J. *et al.* Association of genetic variation in the tachykinin receptor 3 locus with hot flashes and night sweats in the Women's Health Initiative Study. *Menopause* **24**, 252-261 (2017). https://doi.org/10.1097/gme.0000000000000763

41 Franceschi, C., Garagnani, P., Vitale, G., Capri, M. & Salvioli, S. Inflammaging and 'Garb-aging'. *Trends Endocrinol Metab* **28**, 199-212 (2017). https://doi.org/10.1016/j.tem.2016.09.005

42 Pascual, O., Ben Achour, S., Rostaing, P., Triller, A. & Bessis, A. Microglia activation triggers astrocyte-mediated modulation of excitatory neurotransmission. *Proc Natl Acad Sci U S A* **109**, E197-205 (2012). https://doi.org/10.1073/pnas.1111098109

43 Nakamura, Y. *et al.* Prostaglandin EP3 receptor-expressing preoptic neurons bidirectionally control body temperature via tonic GABAergic signaling. *Sci Adv* **8**, eadd5463 (2022). https://doi.org/10.1126/sciadv.add5463

44 Aten, S., Lynch, N., Saper, C. B. & Machado, N. L. S. A brain-body perspective on thermoregulatory adaptation. *Curr Biol* **35**, R1016-r1028 (2025). https://doi.org/10.1016/j.cub.2025.09.023

45 Arruda, A. P., Milanski, M. & Velloso, L. A. Hypothalamic inflammation and thermogenesis: the brown adipose tissue connection. *J Bioenerg Biomembr* **43**, 53-58 (2011). https://doi.org/10.1007/s10863-011-9325-z

46 Zhang, G. *et al.* Hypothalamic programming of systemic ageing involving IKK-β, NF-κB and GnRH. *Nature* **497**, 211-216 (2013). https://doi.org/10.1038/nature12143

47 Rance, N. E. Menopause and the human hypothalamus: evidence for the role of kisspeptin/neurokinin B neurons in the regulation of estrogen negative feedback. *Peptides* **30**, 111-122 (2009). https://doi.org/10.1016/j.peptides.2008.05.016

48 Rometo, A. M., Krajewski, S. J., Voytko, M. L. & Rance, N. E. Hypertrophy and increased kisspeptin gene expression in the hypothalamic infundibular nucleus of postmenopausal women and ovariectomized monkeys. *J Clin Endocrinol Metab* **92**, 2744-2750 (2007). https://doi.org/10.1210/jc.2007-0553

49 Hall, J. E. Neuroendocrine physiology of the early and late menopause. *Endocrinology and Metabolism Clinics* **33** (2004/12/01). https://doi.org/10.1016/j.ecl.2004.08.002

50 Hall, J. E., Lavoie, H. B., Marsh, E. E. & Martin, K. A. Decrease in Gonadotropin-Releasing Hormone (GnRH) Pulse Frequency with Aging in Postmenopausal Women*. *The Journal of Clinical Endocrinology & Metabolism* **85** (2000/05/01). https://doi.org/10.1210/jcem.85.5.6612

51 Christ, J. P., Navarro, V. M. & Reed, S. D. Nonhormonal Therapies for Menopausal Vasomotor Symptoms. *Jama* **330**, 1278-1279 (2023). https://doi.org/10.1001/jama.2023.15965

52 Avis, N. E. *et al.* Duration of Menopausal Vasomotor Symptoms. *JAMA Internal Medicine* **175** (2015/04/01). https://doi.org/10.1001/jamainternmed.2014.8063

53 He, Z. *et al.* Novel insight into the role of A-kinase anchoring proteins (AKAPs) in ischemic stroke and therapeutic potentials. *Biomedicine & Pharmacotherapy* **175**, 116715 (2024). https://doi.org/https://doi.org/10.1016/j.biopha.2024.116715

54 Koster, K. P. *et al.* Akap5 links synaptic dysfunction to neuroinflammatory signaling in a mouse model of infantile neuronal ceroid lipofuscinosis. *Front Synaptic Neurosci* **16**, 1384625 (2024). https://doi.org/10.3389/fnsyn.2024.1384625

55 Sanderson, J. L. & Dell'Acqua, M. L. AKAP signaling complexes in regulation of excitatory synaptic plasticity. *Neuroscientist* **17**, 321-336 (2011). https://doi.org/10.1177/1073858410384740

56 Weisenhaus, M. *et al.* Mutations in AKAP5 disrupt dendritic signaling complexes and lead to electrophysiological and behavioral phenotypes in mice. *PloS one* **5**, e10325 (2010). https://doi.org/10.1371/journal.pone.0010325

57 Engeland, K. Cell cycle regulation: p53-p21-RB signaling. *Cell Death & Differentiation* **29**, 946-960 (2022). https://doi.org/10.1038/s41418-022-00988-z

58 Wagner, K. D. & Wagner, N. The Senescence Markers p16INK4A, p14ARF/p19ARF, and p21 in Organ Development and Homeostasis. *Cells* **11** (2022). https://doi.org/10.3390/cells11121966

59 Wang, L., Lankhorst, L. & Bernards, R. Exploiting senescence for the treatment of cancer. *Nature Reviews Cancer* **22**, 340-355 (2022). https://doi.org/10.1038/s41568-022-00450-9

60 Chinta, S. J. *et al.* Cellular senescence and the aging brain. *Exp Gerontol* **68**, 3-7 (2015). https://doi.org/10.1016/j.exger.2014.09.018

61 Lohff, J. C., Christian, P. J., Marion, S. L. & Hoyer, P. B. Effect of duration of dosing on onset of ovarian failure in a chemical-induced mouse model of perimenopause. *Menopause* **13**, 482-488 (2006). https://doi.org/10.1097/01.gme.0000191883.59799.2e

62 Van Kempen, T. A., Milner, T. A. & Waters, E. M. Accelerated ovarian failure: a novel, chemically induced animal model of menopause. *Brain Res* **1379**, 176-187 (2011). https://doi.org/10.1016/j.brainres.2010.12.064

63 Mayer, L. P., Devine, P. J., Dyer, C. A. & Hoyer, P. B. The follicle-deplete mouse ovary produces androgen. *Biol Reprod* **71**, 130-138 (2004). https://doi.org/10.1095/biolreprod.103.016113

64 Cao, L. B. *et al.* Systemic changes in a mouse model of VCD-induced premature ovarian failure. *Life Sci* **262**, 118543 (2020). https://doi.org/10.1016/j.lfs.2020.118543

65 Cao, L. B. *et al.* Hormone-Like Effects of 4-Vinylcyclohexene Diepoxide on Follicular Development. *Front Cell Dev Biol* **8**, 587 (2020). https://doi.org/10.3389/fcell.2020.00587

66 Hajdarovic, K. H. *et al.* Single-cell analysis of the aging female mouse hypothalamus. *Nat Aging* **2**, 662-678 (2022). https://doi.org/10.1038/s43587-022-00246-4

67 Siletti, K. *et al.* Transcriptomic diversity of cell types across the adult human brain. *Science* **382**, eadd7046 (2023). https://doi.org/doi:10.1126/science.add7046

68 Tadross, J. A. *et al.* A comprehensive spatio-cellular map of the human hypothalamus. *Nature* **639**, 708-716 (2025). https://doi.org/10.1038/s41586-024-08504-8

69 Kreisman, M. J., McCosh, R. B. & Breen, K. M. A Modified Ultra-Sensitive ELISA for Measurement of LH in Mice. *Endocrinology* **163** (2022/09). https://doi.org/10.1210/endocr/bqac109

70 Wang, Q. *et al.* The Allen Mouse Brain Common Coordinate Framework: A 3D Reference Atlas. *Cell* **181**, 936-953 e920 (2020). https://doi.org/10.1016/j.cell.2020.04.007

71 Bray, N. L. *et al.* Near-optimal probabilistic RNA-seq quantification. *Nature Biotechnology 2016 34:5* **34** (2016-04-04). https://doi.org/10.1038/nbt.3519

72 Soneson, C., Love, M. I. & Robinson, M. D. Differential analyses for RNA-seq: transcript-level estimates improve gene-level inferences - PubMed. *F1000Res* **4** (12/30/2015). https://doi.org/10.12688/f1000research.7563.2

73 Frankish, A. *et al.* GENCODE reference annotation for the human and mouse genomes. *Nucleic Acids Res* **47** (2019/01/01). https://doi.org/10.1093/nar/gky955

751 74 Szklarczyk, D. *et al.* STRING v11: protein-protein association networks with increased
752 coverage, supporting functional discovery in genome-wide experimental datasets.
753 *Nucleic Acids Res* **47**, D607-D613 (2019). https://doi.org/10.1093/nar/gky1131
754 75 Piehl, N. *et al.* Cerebrospinal fluid immune dysregulation during healthy brain aging and
755 cognitive impairment. *Cell* **185** (2022/12/12). https://doi.org/10.1016/j.cell.2022.11.019
756 76 El Khoudary, S. R. *et al.* The menopause transition and women's health at midlife: a
757 progress report from the Study of Women's Health Across the Nation (SWAN).
758 *Menopause* **26**, 1213-1227 (2019). https://doi.org/10.1097/gme.0000000000001424
759 77 Jew, B. *et al.* Accurate estimation of cell composition in bulk expression through robust
760 integration of single-cell information. *Nature Communications 2020 11:1* **11** (2020-04-
761 24). https://doi.org/10.1038/s41467-020-15816-6
762

a

Demographics of study subjects		
# of donor tissue		31
Age (years)	mean (min., max.)	53.7 (28, 65)
Body mass index (BMI)	mean (min., max.)	28.6 (20.1, 33,4)
Race, n (%)	Asian	1 (3.2%)
	Black/African American	2 (6.5%)
	White	28 (90.3%)

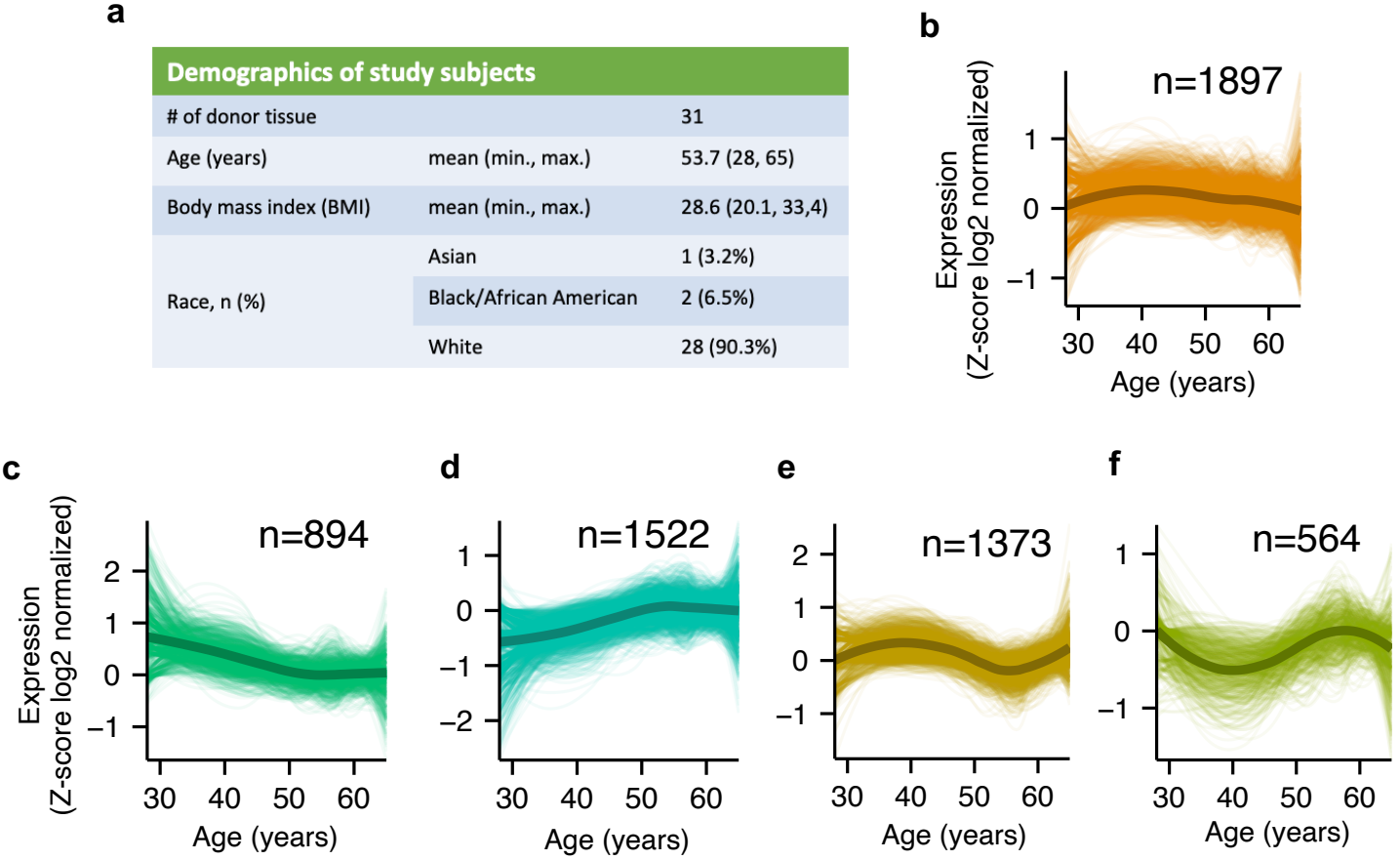

Figure 1. Gene expression trajectories in the human female hypothalamus across chronological age.
a) Demographic overview of the GTEx donor subset used in this study.
b-f) Sets of genes grouped by hierarchical clustering and displayed using LOESS trajectories exhibit distinct patterns, including, **b)** constant expression across age, **c)** decreased expression across age, **d)** increased expression across age, **e)** decreased expression during the menopausal transition, **f)** increased expression during the menopausal transition.

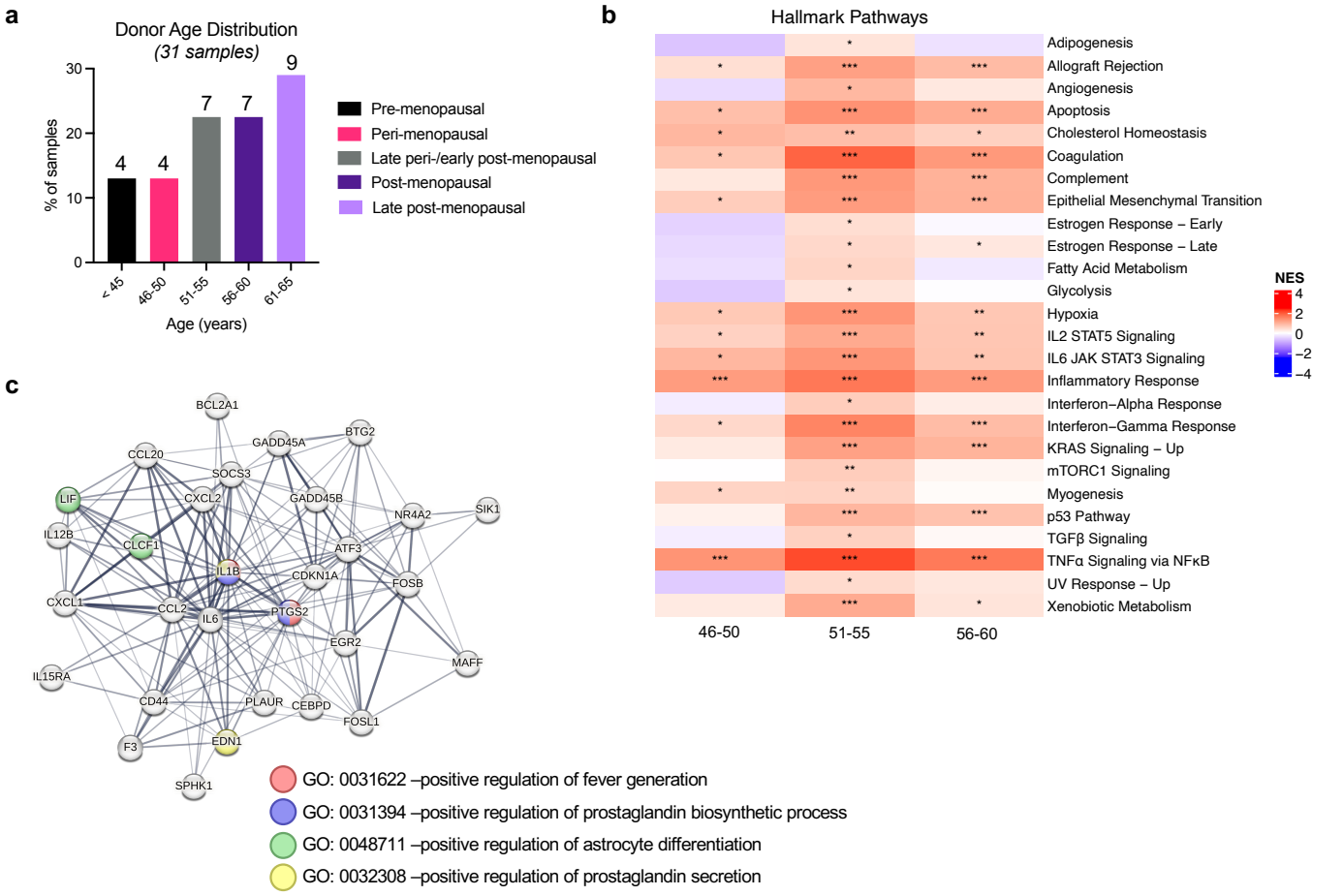

Figure 2. Expression of reproductive- and aging-related genes during the menopausal transition in the human hypothalamus.

a) Distribution of ages within the donor cohort and the defined age groupings for subsequent analyses.
b) Heatmap of normalized enrichment scores (NES) for Hallmark gene sets in which there was a statistically significant pathway enrichment in at least one of the three comparisons; significant enrichments indicated by asterisks (* *p*-adj <0.05; ** *p*-adj < 0.01; *** *p*-adj < 0.001)
c) STRING analysis of TNF-alpha hallmark pathway leading edge genes between the late peri-/early post-menopausal vs. pre-menopausal groups.
d) LOESS trajectories of KNDy genes and their receptors, thermoregulatory genes, astrocyte-, and microglia-marker genes across age in human hypothalamus tissue.

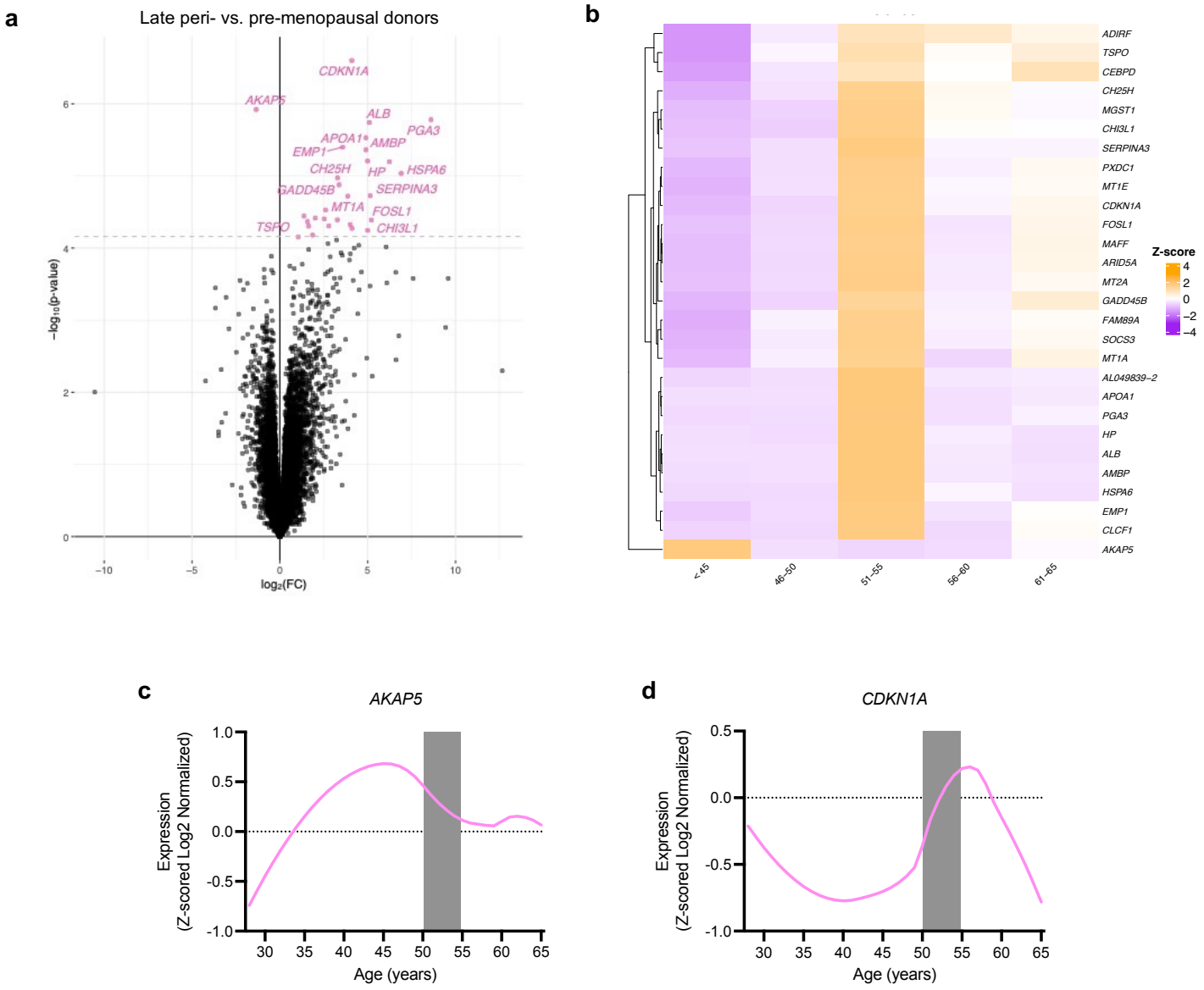

Figure 3. Identification of differentially expressed genes between the late peri-/early post-menopausal donors and the pre-menopausal donors.

a) Volcano plot highlighting significantly differentially expressed genes between late peri-/early post-menopausal and pre-menopausal groups. Genes with a FDR < 0.05 are highlighted in pink.
b) Expression of genes across age groups with a FDR < 0.05.
c) LOESS trajectory of *AKAP5* across age.
d) LOESS trajectory of *CDKN1A* across age.

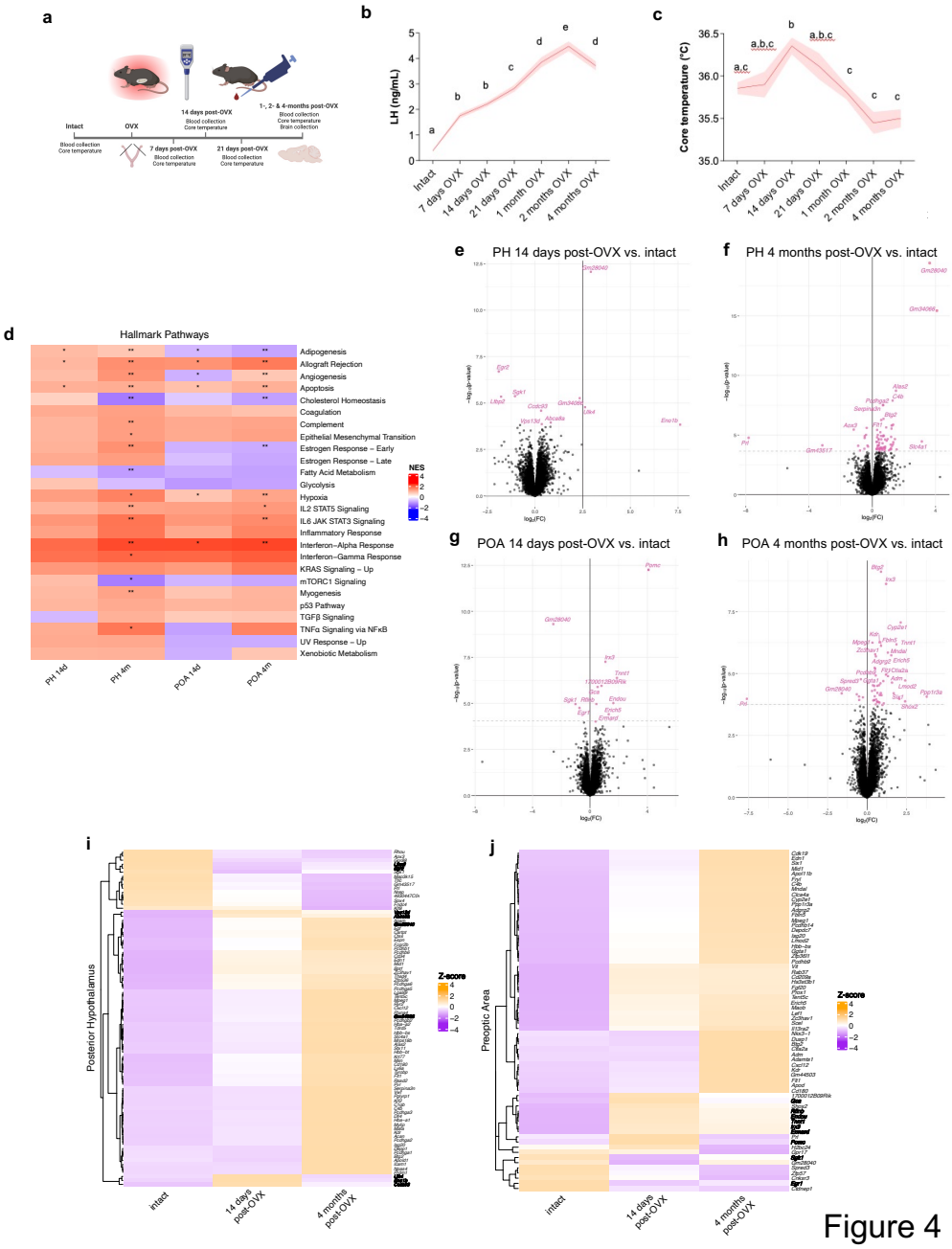

Figure 4

Figure 4. Physiological and transcriptomic changes in post-ovariectomy mouse models recapitulate key features of reproductive aging.

a) Schematic representation of the experimental design.
b) Luteinizing Hormone (LH) concentration in serum isolated from whole blood 7-, 14-, 21-days post-OVX and 1-, 2- and 4-months post-OVX in wild-type female mice (n=20, per condition).
c) Core temperature (ºC) measurements at 7-, 14-, 21-days post-OVX and 1-, 2- and 4-months post-OVX in wild-type female mice (n=20, per condition). b-c) Data values are shown as mean ± SEM. Groups with different letters are significantly from each other, P < 0.05 by One-way ANOVA/Tukey.
d) Heatmap of normalized enrichment scores (NES) for Hallmark gene sets in the Posterior Hypothalamus (PH) and the Preoptic Area (POA); significant enrichments indicated by asterisks (* *p*-adj <0.05; ** *p*-adj < 0.01; *** *p*-adj < 0.001)

e-h) Volcano plots highlighting significantly differentially expressed genes between labeled conditions and regions. Genes with a FDR < 0.05 are labeled in pink.

i) Expression of PH DE genes identified in **b** across conditions.
j) Expression of POA DE genes identified in **d** across conditions.

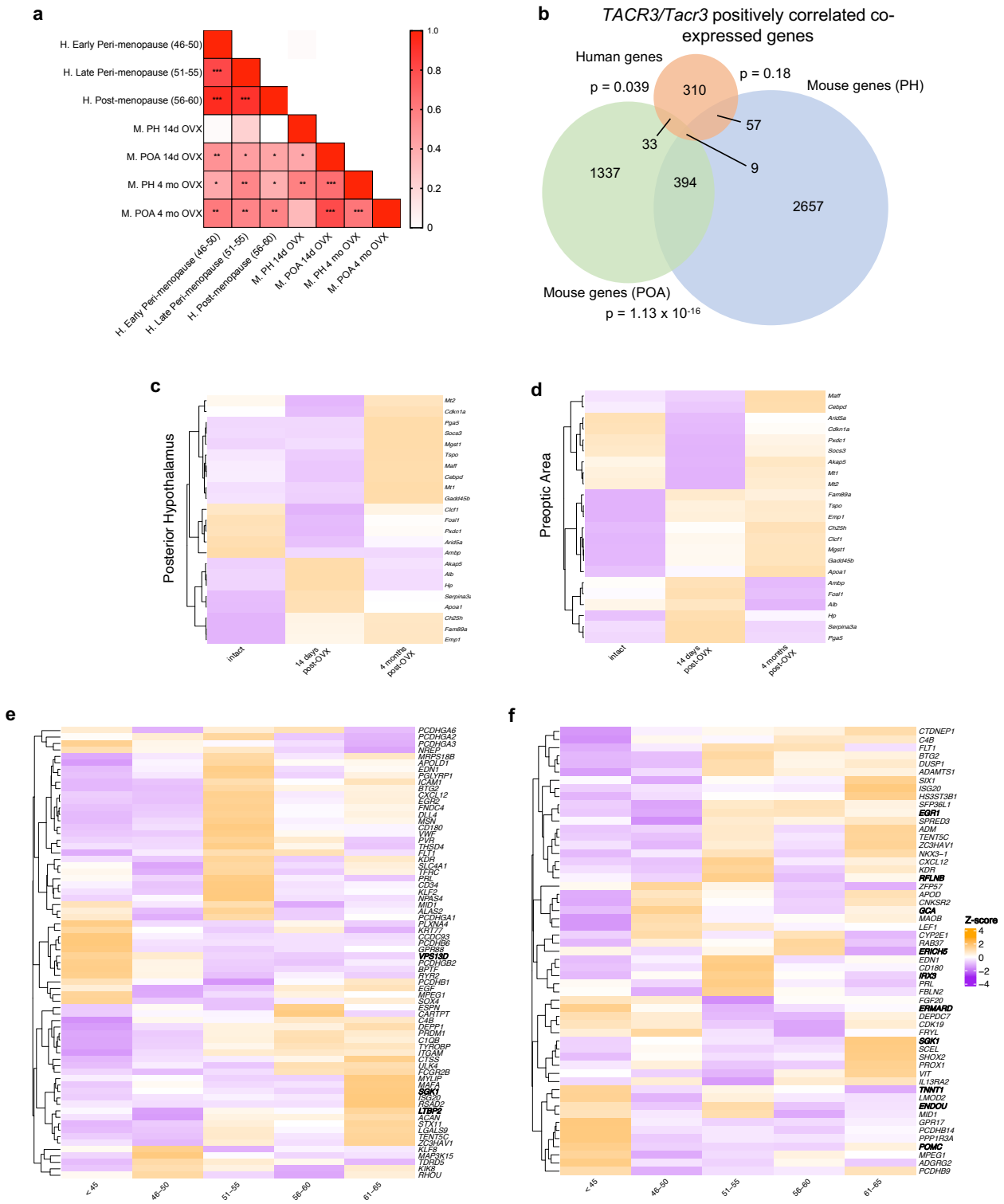

Figure 5. Comparative analysis of human and mouse hypothalamic reproductive aging datasets.

a) Heatmap of GSEA pathway correlations between human and mouse datasets; *p*-value from Pearson's correlation.

b) Overlap of *TACR3/Tacr3* positively correlated co-expressed genes between human and mouse; *p*-value from hypergeometric test.

Expression of identified DE genes from the human dataset across conditions in the mouse **c)** PH and **d)** POA datasets.

e) Expression of identified DE genes from the mouse PH across age groups in the human dataset.

f) Expression of identified DE genes from the mouse POA across age groups in the human dataset.